NATIONAL ADVISORY COMMITTEE FOR AERONAUTICS

TECHNICAL MEMORANDUM

No. 1102

HIGH-SPEED MEASUREMENTS ON A SWEPT-BACK WING

(SWEEPBACK ANGLE $\varphi = 35^{\circ}$)

By B. Göthert

Translation

Hochgeschwindigkeitmessungen an einem Pfeilflugel
(Pfeilwinkel $\varphi = 35^{\circ}$)

Lilienthal-Gesellschaft 156

Washington

March 1947

NATIONAL ADVISORY COMMITTEE FOR AERONAUTICS

TECHNICAL MEMORANDUM NO. 1102

HIGH-SPEED MEASUREMENTS ON A SWEPT-BACK WING (SWEEPBACK ANGLE $\varphi = 35^\circ$)*

By B. Göthert

Abstract: In the following, high-speed measurements on a swept-back wing are reported. The curves of lift, moment, and drag have been determined up to Mach numbers of M = 0.87, and they are compared to a rectangular wing. Through measurements of the total-head loss behind the wing and through schlieren pictures, an insight into the formation of the compression shock at high Mach numbers has been obtained.

OUTLINE

*"Hochgeschwindigkeitmessungen an einem Pfeilflügel (Pfeilwinkel $\varphi = 35^\circ$). From Lilienthal-Gesellschaft fur Luftfahrtforschung, Report 156, pp 30-40.

V. Summary

I. DIMENSIONS OF THE WING MODEL AND SUMMARY OF THE EXPERIMENTS

Stimulated by the AVA investigation[1] on the various swept-back wings an investigation in the DVL high-speed wind tunnel (2.7 meters diameter) has been conducted on a swept-back wing. This investigation is to be considered as a link to the preceding larger systematic series of tests on various swept-back wings. Since the dimensions of the DVL model in comparison to those of the AVA model are considerably larger - for example, the span of the DVL swept-back wing is 1.20m whereas the AVA-Göttingen model was only 0.08m - these results give information primarily at high Reynolds numbers regarding the delaying of compressibility effects by means of sweepback.

The sweepback angle of the model was $\varphi = 35^\circ$ (referred to the $l/4$-line). The aspect ratio was $b^2/F = 6$ and the taper ratio $l_i/l_a = 2$ (fig. 1). The profile used was measured in the flight direction and corresponds to a normal profile without camber and with a 12-percent-thickness ratio [2](NACA 0 00 12-1.1 30). In using this profile it is realized that it is not the most favorable high-speed profile, but it was purposely selected in order to make possible a direct comparison with similar measurements in the DVL high-speed wind tunnel - that is, a comparison with a wing without sweepback and with a

[1] Ludwieg, H. Pfeilflügel bei hohen Geschwindigkeiten, Report 127 of the Lilienthal-Gesellschaft, p. 44.

[2] The designation of Profiles as used in the DVL would be as follows for the example of the NACA 1 30 12-1.1 40:

Max Camber $f/2$ = 1 percent
Position of Max Camber $x_f/2$ = 30 percent of chord behind leading edge
Thickness Ratio = 12 percent
Nose Radius = 1.1 percent
Position of max thickness behind the leading edge $x_d/1$ = 40 percent

normal position of maximum thickness. The Reynolds number based upon the mean chord of the swept-back wing was varied from Re = 1.3×10^6 to 2.6×10^6, which is higher than the Reynolds number at which transition from the laminar to turbulent boundary layer takes place on a flat plate (fig. 1).

The longitudinal moments of the swept-back wing were, as usual, based upon the geometric mean chord $l_m = \frac{\int l y^2 dy}{F}$ and were referred to a moment axis which corresponds to the $l/4$-line of a rectangular wing. In the case of the swept-back wing it corresponds to the neutral-point position of the so defined $l/4$-line of the rectangular wing with a rectangular lift distribution along the span. The location of the moment axis defined in that manner is at a distance $\Delta x_E = 243\text{mm} = 1.19 l_m$ behind the point of the swept-back wing.

At various angles of attack and stream velocities, three-component force measurements were conducted at various Mach numbers as well as were measurements of total-head loss behind the wing, and optical observations using the schlieren method.

II. LIFT, MOMENT AND DRAG OF THE SWEPT-BACK WING

1. Lift

The curves of lift coefficient c_a as a function of angle of attack are shown in figure 2 for several Mach numbers. While at the small Mach number M = 0.30 and 0.55 the curves are straight up to the highest measured angle of attack $\alpha = 8^\circ$, there occurs in the regions of higher lift coefficients, at higher Mach numbers, a continuously increasing curvature which decreases the slope of the lift curve. This curvature begins at the Mach number M = 0.70 and is slightly pronounced at lift coefficients of about $c_a = 0.6$, but is stronger at higher Mach numbers where simultaneously a decrease is brought about in the lift coefficient at which bending occurs; for example, the bending of the lift curve at the Mach number M = 0.87 begins at lift coefficients as low as about $c_a = 0.3$. This loss of lift indicated by the bending

of the curves is always continuous - even at the highest measured Mach numbers and angles of attack it is relatively weak, thus in general it causes no serious danger to the flight characteristics.

On the plots of $c_a = f(\alpha)$, the lift curve at the smallest Mach number is shown on all of them for purposes of comparison, thereby showing that the slope of the lift curve at small angles of attack is steeper. This also is very well shown in figure 3, where $\delta c_a/\delta\alpha = f(M)$ has been plotted. It is seen that the measured curves at small lift coefficients near $c_a = 0$ are even a little bit steeper than what the theory would require for a sweepback angle of 35° and an aspect ratio of 6. It must be emphasized here that the theoretical curves for compressible flow are based upon the equivalent incompressible flow. Thus it is assumed that the incompressible flow about a swept-back wing with finite aspect ratio is known; this known incompressible flow, however, is at present not completely adequate, so that in certain circumstances this explains the observed differences[3]. As is shown later, a difference occurs between the lift slope $\delta c_a/\delta\alpha$ of the rectangular and the swept-back wing even in incompressible flow, which indicates the existence of a deficiency in the theoretical analysis of the flow about a swept-back wing.

The continuous increase in the slope of the lift curve $\delta c_a/\delta\alpha$ with increasing Mach numbers as shown in figure 2 for lift coefficients near $c_a = 0$ occurs up to Mach numbers of $M = 0.82$ for $c_a = 0.3$ and up to $M = 0.70$ for $c_a = 0.55$. At higher Mach numbers the curves bend to lower values, as has already been shown by the curves of $c_a = f(\alpha)$. The loss in lift shown by the different lift curves in the regions at higher Mach numbers and lift coefficients is, as usual, traced to the fact that the velocity of sound is locally exceeded and compression shock and flow separation results.

[3]Weissinger "Der schiebende Tragflügel bei gesunder Strömung", Report S2 of the Lilienthal-Gesellschaft.

Multhopp "Anwendung der Tragflügeltheorie auf Fragen der Flugmechanik", Report S2 of the Lilienthal-Gesellschaft.

2. Moment

The instability of lift already observed is reflected in the curves of the longitudinal-moment coefficient $c_m = f(c_a)$ and it appears to a greater extent here (fig. 4). Thus, if a certain high-lift coefficient is exceeded, the principal result is a sudden break in the moment curves in the direction of tail-heavy moments; this critical lift coefficient decreases with increasing Mach number. The break in the moment curve in the tail-heavy sense evidently is caused by separation phenomena at the wing tips, which for the swept-back wing originates and is aided by the outward flowing boundary layer.

In the region of small lift coefficients it is seen that up to a Mach number of $M = 0.70$ the moment curves are not changed, and that apart from a slight displacement the moment curves are scarcely changed even up to $M = 0.80$. At the highest measured Mach numbers $M = 0.85$ and 0.87 the moment curves even at small lift coefficients turn to a nose-heavy, that is, a stable direction, which is indicated by the loss of lift at the wing center. These observations made at small angles of attack are in accordance with the following considerations given in section IV, according to which at small angles of attack compression shock and separation phenomena are first precipitated at the wing center. At higher lift coefficients $c_a > 0.4$, at which the moment measurements result in a break in the tail-heavy sense, there also occur additional disturbances evidently brought about by the incidence which results in boundary-layer accumulation at the wing tips, so that the flow there separates particularly strong, bringing about the observed changes in the moments. *

The position of the neutral point $\delta c_m/\delta c_a$ indicated by the trend of the moment curves is shown for various lift coefficients in figure 3. One clearly sees that in spite of the increasing velocities up to Mach numbers of $M = 0.80$, the position of the neutral point is not changed in the regions of small lift coefficients near $c_a = 0$, and when the Mach number is increased beyond $M = 0.80$ the shift in the neutral point curves in the stable direction. At high lift coefficients $c_a = 0.5$ a strong destabilizing shift in the position of the neutral point occurs with increasing Mach number, which is shown by the strong break in the moment curves beyond the critical lift coefficient.

3. Drag

The curves of drag coefficient c_w as a function of lift coefficient c_a are shown in figure 5 for several Mach numbers. The first significant drag increase over those values for low velocities corresponds to the break in the curve at $c_a = 0.4$ and at a Mach number $M = 0.70$. At the higher Mach numbers $M = 0.80$ or $M = 0.84$ the drag increase occurs at the lower lift coefficients of $c_a = 0.3$ and $c_a = 0.15$, respectively, while at the highest Mach number $M = 0.87$ a considerable drag increase is noticed even in symmetrical flow ($c_a = 0$).

Here also the cause of the increase in drag at high Mach numbers and lift coefficients is attributed to the formation of compression shocks and the resulting separation of the boundary layer.

III. COMPARISON BETWEEN THE SWEPT-BACK WING AND THE RECTANGULAR WING

In order that the advantages to be obtained by sweepback at high velocities can be evaluated, they are compared to the results previously reported on the high-speed measurements of a rectangular wing of the same profile NACA 0 00 12-1.1 30. This wing which is used for comparison likewise has an aspect ratio $b^2/F = 6$; however, its plan form is not trapezoidal but is rectangular and hence has a constant chord.

1. Lift and Moment

In figure 6 the lift and moment curves of the swept-back and the rectangular wing are compared at Mach numbers $M = 0.30$, 0.75, and 0.87. At the smallest Mach number $M = 0.30$ the swept-back wing exhibits a smaller lift-curve slope than does the rectangular wing. The direction of this deviation is indeed in accordance with theory; however, the magnitude is not, since the decrease in the slope of the lift curve $\delta c_a/\delta \alpha$ due to sweepback, by no means corresponds to the ratio of $\cos \varphi$ which is the main term governing the decrease. While the lift curves for the swept-back wing and also the rectangular wing are straight, the moment curves of the swept-back

wing, however, bend slightly even at small Mach numbers whereas those of the rectangular wing do not.

The occurrence of strong instability at the Mach number $M = 0.75$ is retarded from $c_a = 0.4$ to $c_a = 0.6$ and in the moment curves even from $c_a = 0.18$ to $c_a = 0.45$ by means of sweepback. The advantages obtained by sweepback are still evident at the highest measured Mach number $M = 0.87$ at which the beginning of the instability in the lift and the moment curves is displaced from $c_a = 0.1$ to $c_a = 0.3$.

The comparison of the slope of the curves $\delta c_a/\delta\alpha$ as a measure of the lift increase and $\partial c_m/\partial c_a$ as a measure of the position of the neutral point shows (fig. 7) for the regions of small lift coefficients that the rough disturbance of the lift slope does not occur at all for the swept-back wing up to the limit $M = 0.89$ of the measurements, and that the position of the neutral point is first effected upon exceeding the Mach number $M = 0.80$. In the case of the rectangular wing these instabilities occur at $M = 0.80$ for the lift slope and at $M = 0.73$ for the position of the neutral point.

It is emphasized that the neutral point of the swept-back wing is in no way shifted at small lift coefficients up to the beginning of the disturbances at the Mach number $M = 0.80$, while the rectangular wing with the particular profile employed shows a continuous shift of the neutral point in an unstable direction as the Mach numbers increase; that is, a shift toward the leading edge of the wing. This phenomenon may be explained by the fact that the shift of the neutral point of a rectangular wing in the forward direction is counteracted by a rearward shift of the neutral point which is evidently brought about by the center of pressure of lift forces which is displaced in the direction toward the wing tips. A certain outward displacement of the center of pressure of the lift forces is also established by the requirements of the Prandtl rule, since the equivalent incompressible flow has a larger sweepback angle, which according to the calculations of Multhopp and Weissinger results in an outward shift of the lift distribution.

2. Drag

The drag coefficient of the swept-back wing and the rectangular wing is plotted for constant values of lift

coefficient $c_a = 0$, 0.2, and 0.4 as a function of the Mach number in figure 8. From this it is seen that for the lift coefficients considered, the increase in drag of the swept-back wing is displaced approximately $\Delta M = 0.08$ to higher Mach numbers; for example, at a lift coefficient $c_a = 0$ the drag increase of the rectangular wing breaks at a Mach number of about $M = 0.72$ and that of the swept-back wing breaks at $M = 0.80$. This displacement of the drag increase with reference to Mach number affords an advantage due to sweepback which amounts to this value of $\Delta M = 0.08$.

It is to be noticed further that, especially at the lift coefficients $c_a = 0$ and 0.2, the drag increase upon exceeding the critical Mach number is evidently less steep in the case of the swept-back wing than in the case of the rectangular wing. The explanation for this different behavior in the slope of the drag curve may be traced to the fact that in the case of the swept-back wing the compression shock first occurs only at the wing portions near the wing center, and from there it gradually spreads outward over the entire span (see section IV).

If by using sweepback on a model wing a considerable advantage is to be obtained over that of the wing without sweepback, then the question arises whether the magnitude of the advantage corresponds approximately to that required by theory, or whether for example through disturbing influences of adjacent bodies an essential deduction is brought about. To answer this question measurements on another purposely selected model wing at small velocities were conducted, from which the essence of the sweepback effect is clearly visible. A rectangular wing with profile NACA 0 00 15-1.1 40 was set obliquely to the direction of the flow thereby simulating the action of wings with sweepback. It was placed in the air jet of a wind tunnel and the pressure distribution at the center section of the wing was measured at various attitudes by means of a number of pressure orifices (fig.9). By means of this experimental apparatus the flow behavior about an infinitely long rectangular wing was simulated to a close approximation at the wing center section which was inclined at a fixed angle with respect to the direction of the stream. In a frictionless flow with such an arrangement, only the velocity component perpendicular to the leading edge of the wing has an effect on the forces, while the component parallel to the leading edge of the

wing only augments the friction over the top surface thereby resulting in secondary forces which transport the boundary layer spanwise along the wing. At a fixed angle of attack measurements were taken in a plane perpendicular to the leading edge of the wing; the pressures on the wing vary as the square of the effective velocity, that is as $\cos^2\varphi$, where φ designates the angle between the section and the direction of the undisturbed flow. This law is confirmed in figure 9 where the measured points for the angles of attack of 0°, 4°, and 8° are shown. In this figure the individual circles are the measured points, whereas the solid curves for sweepback angles other than 0° were obtained by multiplying those values for $\varphi = 0°$ by the factor $\cos^2\varphi$.

According to these considerations a two-fold effect of the oblique wing is to be expected at high velocities. First due to the decrease of the velocity corresponding to the $\cos^2\varphi$-law the velocity of sound is first attained on the profile at higher Mach numbers than in the case of the wing[4] perpendicular to the flow direction. Furthermore the line of the largest additional velocity parallel to the leading edge of the wing is inclined with respect to the free-flow direction and it is expected, therefore, that the compression shock front is also inclined to the direction of flow by the same angle. Since compression shocks are only possible if the velocity component perpendicular to the shock plane is larger than the velocity of sound, a compression shock on an oblique wing can first occur when the velocity component perpendicular to the leading edge of the wing locally exceeds the velocity of sound; that is, aside from the local additional velocities the Mach number of the stream in the case of compression shock and therewith also the accompanying disturbing phenomena which are made possible are increased in the ratio $1/\cos^2\varphi$ when changing to the wing normal to the flow direction.

On the basis of these considerations it must also be possible to obtain the same curves for the forces, for example $c_a = f(M)$, independent of the oblique angle, provided one increases the force coefficients in the ratio $1/\cos^2\varphi$ and decreases the Mach number by the factor $\cos\varphi$.

[4]B. Göthert "Berechnung des Geschwindigkeitsfeldes von Pfeilflügeln bei hohen Unterschallgeschwindigkeiten", Report 127 of the Lilienthal-Gesellschaft, p. 52.

In the case of drag, the drag coefficient drops in the first approximation so that only the decrease in the Mach number by the factor cos φ has an effect. In so doing, it is not considered in this simple manner that the effective local Mach number also is decreased by decreasing the local additional velocity (fig. 9) and therefore the distortion of the Mach number scale must be even stronger than the factor cos φ.

In the first approximation for the swept-back wing, if one assumes that this law is valid as has previously been demonstrated for the oblique wing, then, for example, the drag curves for the rectangular and for the swept-back wing must be brought approximately to the same level provided the reduced Mach number M cos φ instead of the Mach number is used for plotting. As a result of not considering the additional velocities in the foregoing distortion it was found that in spite of what was expected, the increase in drag of the swept-back wing occurred at a lower reduced Mach number than did the rectangular wing. The curves according to this scheme are shown in figure 10 and they show the opposite position of the curves for swept-back and rectangular wings. The curves for the swept-back wing do not lie at larger reduced Mach numbers than do the rectangular wings but instead they lie at a significantly lower reduced Mach number. The advantages to be obtained through sweepback, therefore, are less than what theoretical consideration would require for an oblique wing.

Since the changes are adverse with regard to the behavior of the flow about an oblique wing, it is to be expected that at the wing center the sweepback effect does not completely occur, and thus brings about for the most part the observed decrease in the effect of sweepback. Furthermore, as a result of the three-dimensional flow about the wing tips, it happens that without sweepback the wing tips show a more favorable behavior than other wings, thus preventing the full advantages of sweepback to be obtained. Through additional measurements and schlieren observations the flow behavior at the center of a swept-back wing was quite closely investigated.

IV. SPECIAL INVESTIGATIONS FOR CLARIFYING THE PREMATURE DRAG RISE ON THE SWEPT-BACK WING

1. Oblique Wings with End Plates Tested at Small Velocities

An investigation at small velocities shall first be reported which furnishes an insight into the behavior of the incompressible flow about the center part of a swept-back wing. Since for reasons of symmetry the same streamlines at the center of a swept-back wing must exist as in the case of plane flow, whereas at larger distances from the wing center a more or less strongly cambered flow surface can exist, then the flow produced by the symmetry of the swept-back wings can easily be simulated. The wing already referred to in figure 9 was fitted with a flat plate (fig. 11). By means of pressure-distribution measurements at various distances from this plate, the flow produced by this plate can be determined. In a preliminary experiment a normal wing was first tested, that is, a wing with a sweepback angle of 0°, and it was demonstrated that the plate at this attitude exerted no noticeable influence on the pressure distribution. For the wing inclined at the angle $\varphi = 45^\circ$ there resulted, however, a considerable disturbance as is shown in detail in figure 11 for the angles of attack $\alpha = 0^\circ$ and 4°. In the immediate vicinity of the plate the under pressure was increased so much that it exceeded the maximum value obtained by the wing normal to the flow direction. According to the measurements this additional under pressure diminishes quite rapidly as the distance from the end plate is increased; in compressible flow this decaying with increasing Mach number is slower, so that the disturbances produced by the wing symmetry occur over the larger part of the wing span. It is therefore established that, especially at high velocities, a considerable hindrance of the sweepback effect occurs at the center of the wing, which provides the cause for the decreased effectiveness of sweepback which was observed in the high-speed measurements.

It is emphasized that these measurements in incompressible flow hold good for a forward swept wing. The corresponding measurements for a swept-back wing would be obtained if the respective position of the end plate was changed. In spite of this it can already be concluded from these measurements that also for the swept-back wing a considerable disturbance of a flow at the wing center is produced.

2. Measurements of Total-Head Loss on the Swept-Back Wing at High Velocities ($\alpha = 0^\circ$)

In order to point out the sweepback effect is hindered at the center of a swept-back wing (fig. 1), the total-head loss was measured behind the swept-back wing at high velocities and at various sections along the span. These measurements were taken at a distance $x = 5.3l_i$ behind the reference axis of moments for the swept-back wing (l_i = wing chord at the wing center). The results of these measurements are shown in figure 12 in which at the Mach number $M = 0.65$ the velocity of sound is not yet exceeded for the zero angle of attack. It is seen that in spite of the unfavorable behavior of velocity at the wing center it is precisely this location at which the smallest integrated total-pressure losses occur, and consequently also the smallest local drag coefficients. The explanation for this is that as a result of the transverse pressure drop in the flow direction the boundary layer is induced outward from the center section and separates at the sides; it therefore stimulates, or to a certain degree, results in a corresponding decrease in drag at the center section. These measurements, clearly show an advantage of the swept-back wing in comparison to the swept forward wing, since the separation which in general is dangerous at the wing-fuselage juncture is retarded by the lateral inducing of the boundary layer. The loss in total pressure at high Mach numbers is shown in figure 14 for the wing center section and in figure 13 for a section at a lateral distance of $0.9l_i$. It is seen that for the section $0.9l_i$ away from the center the first weak compression shock is visible at the Mach number $M = 0.85$, which is indicated by the strong lateral extention of the losses into the free flow. By increasing the Mach number to $M = 0.90$ this lateral extension into the free flow is much stronger as a result of the increased compression shock; however, a pronounced separation is still not noticeable in these curves. In opposition to this, the curves corresponding to the wing center show that at a Mach number of about 0.85 the compression shock already causes the flow to strongly separate. In this case these curves no longer show the sharp division between the friction losses (center point of the curves) and the loss which results from the compression shock (lateral extension of the curves), but instead, both regions are merged together.

Also the friction drag as a result of the premature separation of flow evidently is somewhat lowered. The measurements of total-head losses therefore confirm the concept that, because of the flow symmetry, separation results which gradually spreads over the whole wing.

3. Schlieren Observations[5]

If corresponding to the foregoing developement the compression shock forms first at the wing center in the case of the swept-back wing, whereas at a sufficient distance from the wing center a shock-free transition from supersonic flow to subsonic flow results, then the schlieren method can be suitably used in order to make the shock formation visible. The flow field about a swept-back wing is indeed an unfavorable condition for schlieren observations, since in general only plane and not three-dimensional flow processes can be made visible with the schlieren method. This can be very well illustrated by the schlieren pictures of figure 15 which are for a Mach number at which compression shocks are visible; however, the main question of the position of the shock along the wing span cannot be answered. By means of an artifice, however, it is possible to obtain a good insight into the position of the compression shock as well as into the formation of the supersonic field of the flow about the wing. As is shown in figure 16, grooves were made at various sections along the span of the wing, thereby making the supersonic velocities visible by means of the Mach waves which are emanated. One sees quite clearly that for section I, which is closest to the wing center (center distance = $0.56l_1$), the Mach waves are evident which indicates a supersonic field in the vicinity of this section at the Mach number $M = 0.85$. At the next outward lying section II (mean distance $=1.05l_1$) Mach waves are only very weak and at the outermost section III (center distance = $1.79l_1$) no Mach waves at all are visible. From this picture of the Mach waves it is therefore demonstrated that at large distances for the center section the sonic velocity is not exceeded locally at a free-stream Mach number $M = 0.85$, whereas the center section at the same Mach number a pronounced supersonic field is observed.

[5]The schlieren photographs were taken by F. Mirus in the DVL high-speed wind tunnel.

This phenomena of the supersonic field at the wing center is even more evident at a Mach number $M = 0.875$ (fig. 17) where it is shown to be strengthened. While at the Mach number $M = 0.875$ only very weak Mach waves are visible at the outermost section (center distance $1.79l_i$), at the higher Mach number of $M = 0.89$ the Mach waves at this section are clearly visible (fig. 18). This shows, however, that the Mach waves at the outer sections do not terminate in compression shocks like the supersonic field usually does. Evidently this corresponds to the theoretical considerations of shock-free transition from supersonic flow to subsonic flow, as is shown by these schlieren pictures for sufficient distances from the center portions of the wing.

The schlieren pictures of the outer sections show that, in contrast to the inner sections, especially at those distances less than $0.56l_i$ from the center, the flow does not result in a strong compression shock in the supersonic field.

From the schlieren pictures it is therefore confirmed that for the investigated swept-back wing the strong compression shocks occur at the wing center, while at the wing sections further out the supersonic flow is evidently transformed into subsonic flow without the occurrence of shock.

4. Favorable Fuselage or Nacelle Shapes

The disturbances at the center of the swept-back wings developed as a consequence of the flow symmetry are connected with a corresponding three-dimensional flow. However, if a swept-back wing with a fuselage located at the center is used instead of the swept-back wing alone, it appears possible by means of properly shaping the fuselage to avoid the disturbances at the wing center and therefore produce a favorable behavior. On the basis of these considerations it can be concluded that if a plate which conformed to the streamlines of the distorted flow was placed on the wing (that is, the plate is imagined to be a solidified stream surface), then the plate would exert no effect. Now if one shapes the side of the fuselage in a corresponding manner, then the disturbance brought about by the symmetry of the swept-back wing is decreased and only the effect of the increased local

additional velocity resulting from the fuselage flow would exist. With a fuselage formed according to these viewpoints it is conceivable that a swept-back wing with fuselage would behave considerably better than an isolated swept-back wing. That the advantages can be obtained in this manner is shown by the considerations of figure 10 with regard to the disturbances brought about by wing symmetry.

It is emphasized, however, that fuselages formed according to the above thoughts would be good only for a fixed flight condition while for other flight conditions the best behavior would require other fuselage forms and the first would no longer give the optimum behavior.

In a corresponding manner these considerations hold true also for swept-back wings with nacelles, which, according to AVA-Göttingen experiments are unfavorable when the usual nacelle forms are employed. Such experiments have already, for a long time, been in preparation at the DVL high-speed wind tunnel; however, the models already completed have not yet been investigated because of the extensive engagements of the wind tunnel.

V. SUMMARY

1. High-speed measurements up to a Mach number of $M = 0.87$ have been reported for a swept-back wing with a 35° sweepback angle ($b^2/F = 6$, $l_i/l_a = 2$, profile NACA 0 00 12-1.1 30).

2. Up to a Mach number of $M = 0.80$ no disturbance in lift and moment curves is noticed for a small lift coefficient while at higher lift coefficients ($c_a > 0.4$) the slope of the lift curve $c_a = f(\alpha)$ decreases, but above all, the moment curve strongly breaks towards the tail-heavy direction.

3. At Mach numbers above $M = 0.80$ and up to $M = 0.87$ another disturbance is formed primarily in the moment curve, which in the region of small lift coefficients brings about a displacement of the neutral point in a stabilizing direction, whereas at higher lift coefficients the break already observed at smaller Mach numbers in the stable direction still remains.

4. By 35° of sweepback on a wing a considerable delaying of the compressibility burble to higher Mach numbers can be obtained (amounting to about $\Delta M = 0.08$). This advantage, however, is somewhat less than that which would be expected from theoretical considerations.

5. By means of additional measurements and schlieren observations, it could be shown that the compressibility burble occurred first at the wing center, in which the sweepback effect is diminished because of the symmetry. By forming the sidewalls of the fuselage in the proper manner it can be expected that the burble at the wing center can be extensively avoided, so that swept-back wings with suitably shaped fuselages can behave very much better than the swept-back wing without the fuselage.

DISCUSSION

Ruden: In order to explain the diminished effect of sweepback at the center of the rearward swept wing, Göthert has used pressure-distribution measurements on an oblique wing. This wing has at its center a plate parallel to the flow direction and the horizontal axis. The section on which measurements were taken is in the forward half of the wing. As one can see by the reflections on the plate (see fig. 1) this arrangement can be compared only with a swept-forward wing. The rearward swept wing, on the other hand, corresponds to pressure-distribution measurements on the rearward lying half of the oblique wing (fig. 2).

Pressure-distribution measurements at low velocities have shown that an increase of the point of under pressure near the profile nose at the center of the swept-back wing occurs only for a forward swept model. In the case of a rearward swept wing this under-pressure point is not formed close to the center wall (see fig. 3).

Since a similar behavior can be expected at higher velocities the explanation given by Göthert must be accepted with much foresight. It appears necessary to extend the above selected pressure-distribution measurements to the rearward lying half of the oblique wing.

Göthert: As I have mentioned in my paper, the measurements on the oblique wing with a plate installed on

it which corresponds to the rearward swept wing were provided for in the program; however, on account of the necessary apparatus which has to be constructed, they can not as yet be conducted.

Added in the proof:

The differences in pressure distribution of a forward and a rearward swept wing as shown by Ruden are evidently explained by the theoretical investigations (for example those of Weissinger) of a rearward swept wing and a forward swept wing - the former possessing a drop and the latter a hump in the lift distribution at the wing center. In the case of wings at small angles of attack, however, it is not the lift but the finite wing thickness which determines the additional velocity. In this regard, the available calculations of the additional velocity due to finite wing thickness easily illustrate that in the first approximation it is immaterial whether the wing is swept forward or rearward. In the case of potential flow the direction of flow can be reversed without changing the pressures. By reversing the flow direction the sweepback changes from forward to rearward and vice versa.

Translation by Dean R. Chapman
National Advisory Committee
for Aeronautics.

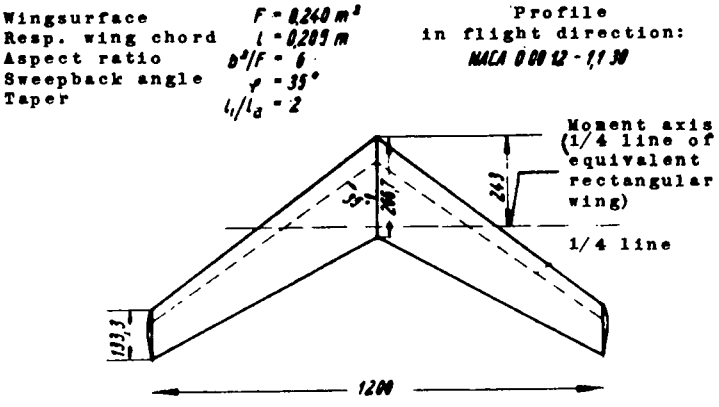

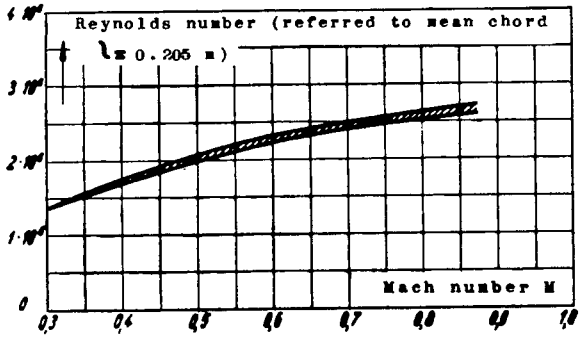

Figure 1. Dimensions of the wing and Reynolds number for high speed measurements on the sweptback wing.

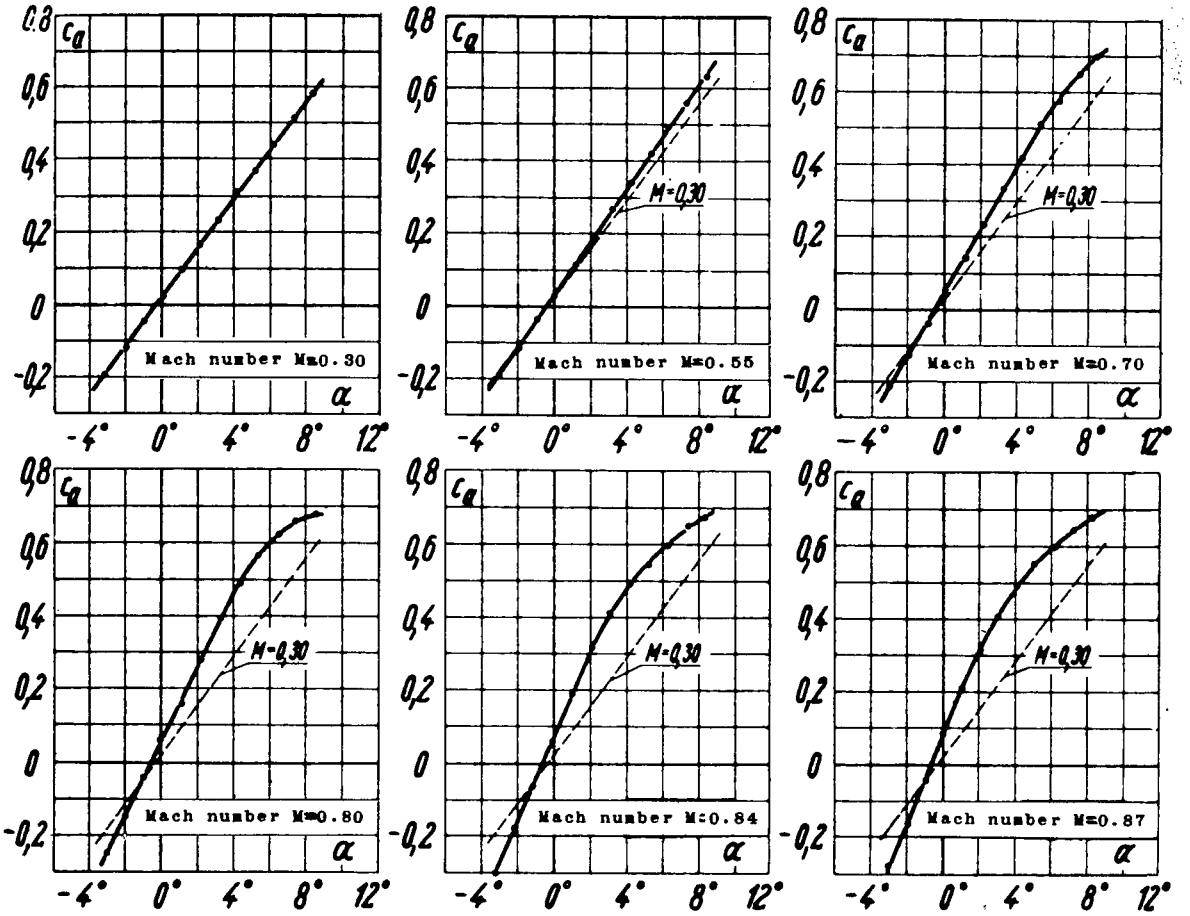

Figure 2. Lift coefficient as a function of angle of attack on a sweptback wing for different Mach numbers.

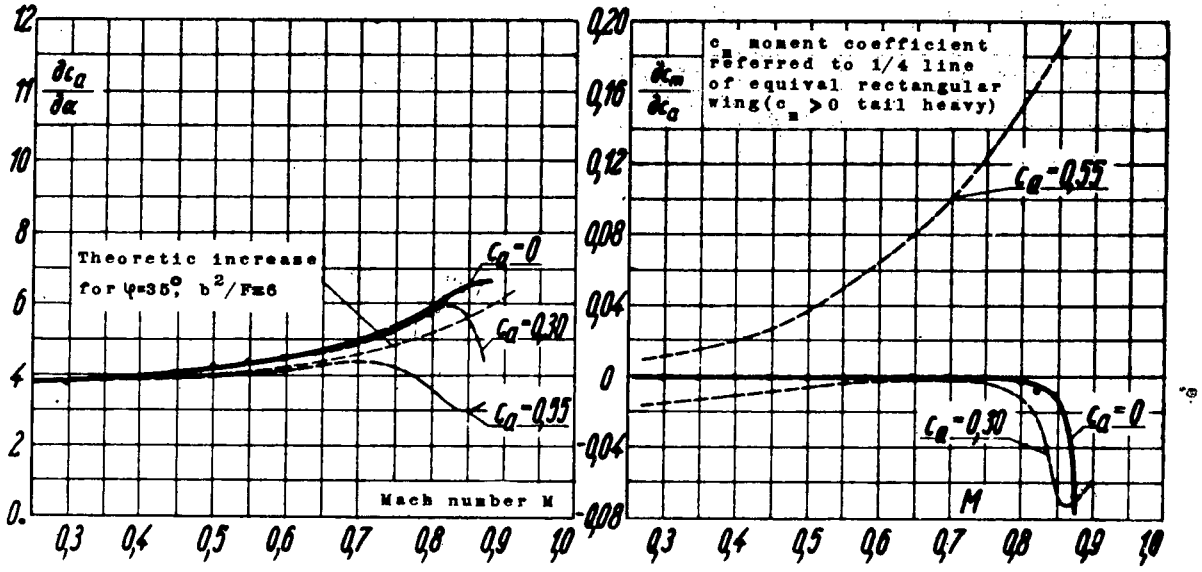

Model wing:

Profile NACA 0 00 12-1.1 30 Aspect ratio $b^2/F=6$

Sweepback angle $\varphi = 35°$ Taper $l_i/l_a = 2$

Figure 3. Increased lift-slope $\delta c_a/\delta \alpha$ and position of the neutral point $\delta c_m/\delta c_a$ of a sweptback wing at high Mach numbers.

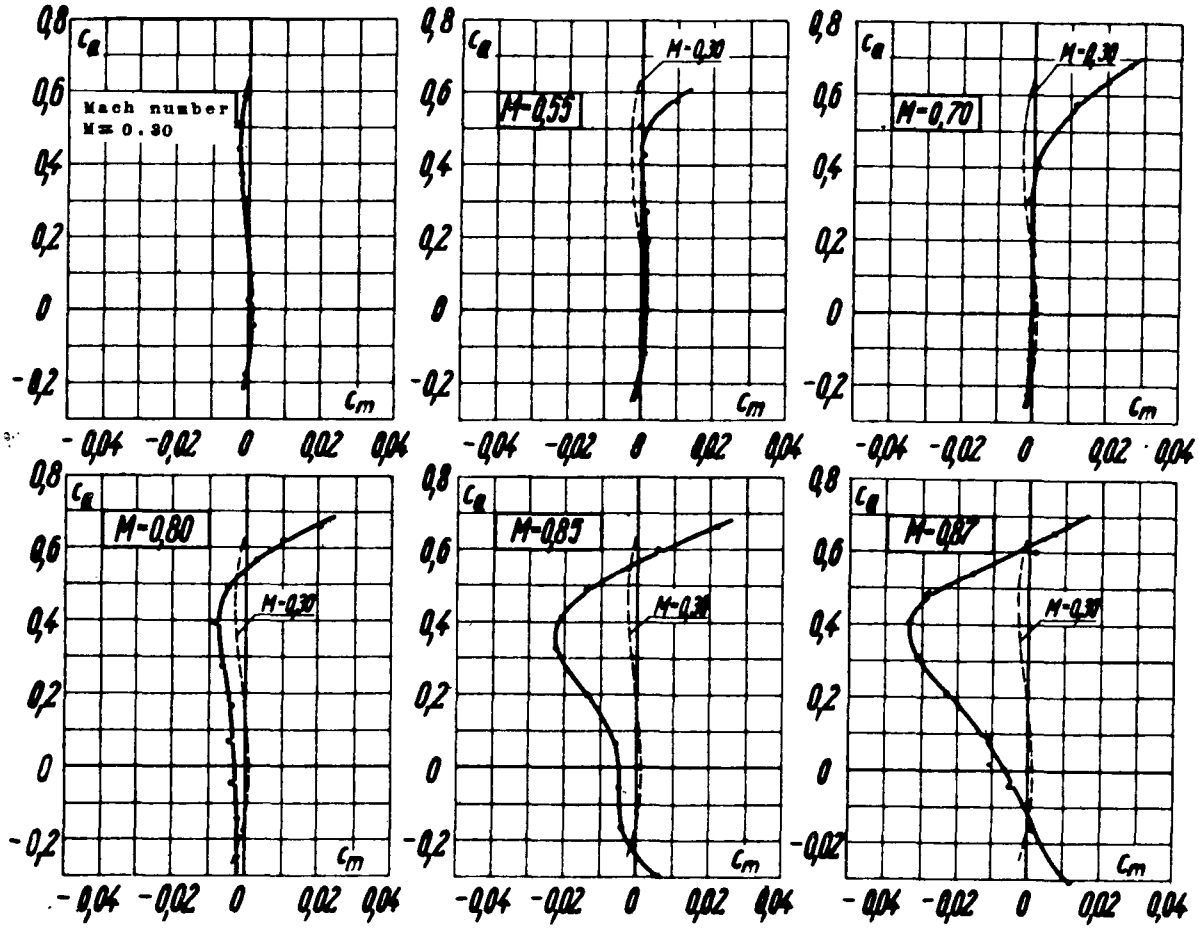

Figure 4. Moment coefficient c_m as a function of the lift coefficient c_a in a sweptback wing at different Mach numbers.

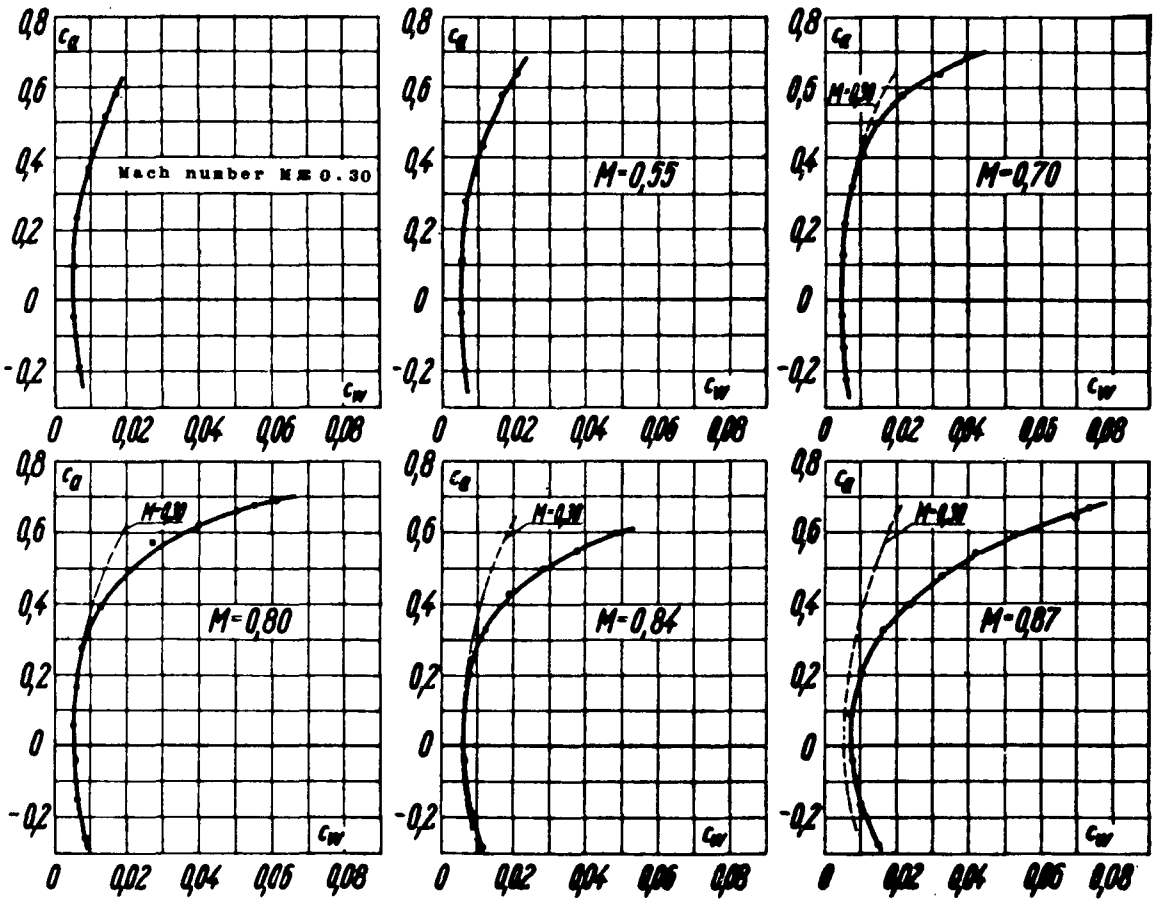

Figure 5. Drag coefficient c_w as a function of the lift coefficient c_a in a sweptback wing at different Mach numbers.

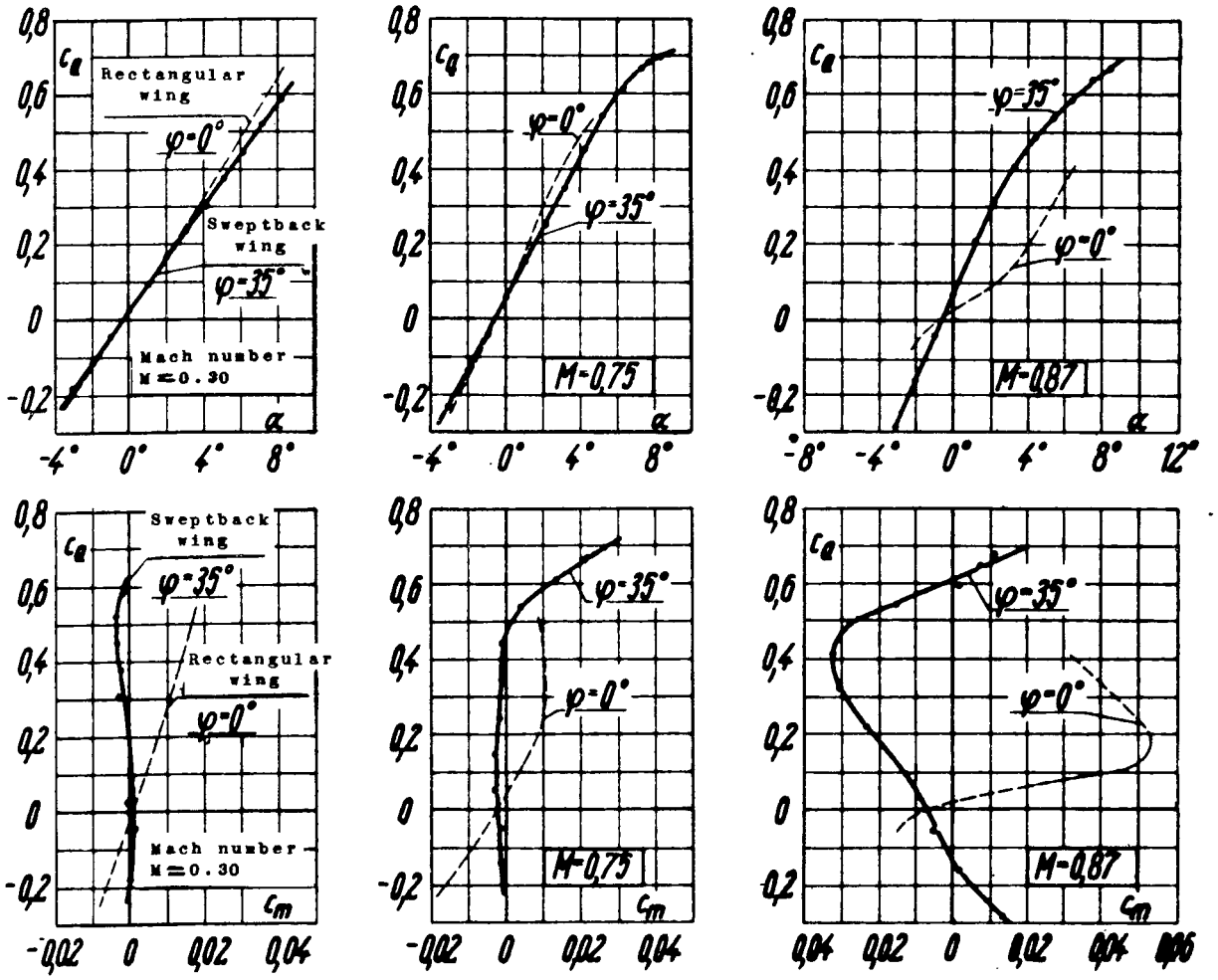

Figure 6. Lift and moment coefficients of a rectangular wing and a sweptback wing at different Mach numbers.

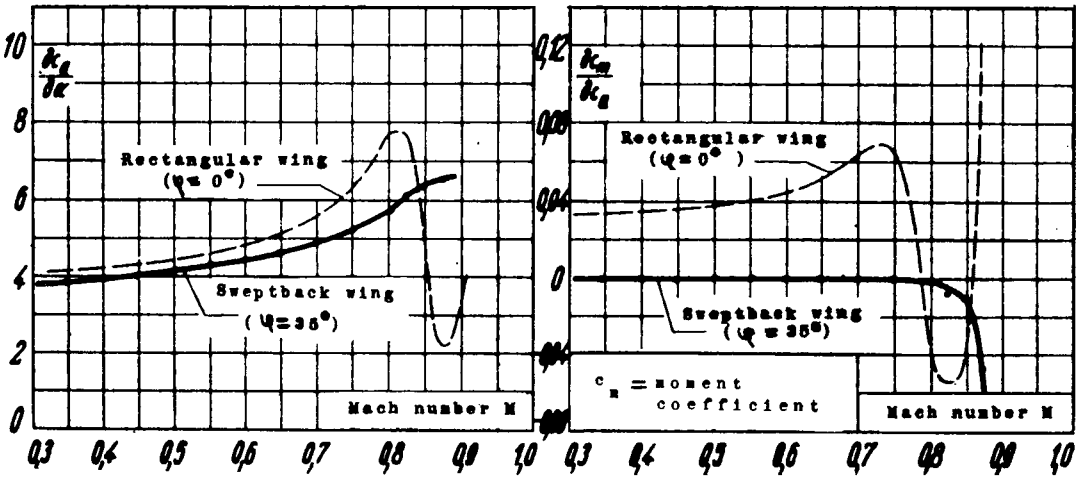

Sweptback wing:

Sweepback angle $\varphi = 35°$

Aspect ratio $b^2/F = 6$

Taper $l_i/l_a = 2$

Profile NACA 0 00 12-1.1 30

Rectangular wing:

$\varphi = 0°$

$b^2/F = 6$

$l_i/l_a = 1$

Profile NACA 0 00 12-1.1 30

Figure 7. Increased lift slope $\delta c_a/\delta\alpha$ and position of the neutral point $\delta c_m/\delta c_a$ of a rectangular wing and of a sweptback wing for the regions of small lift coefficients.

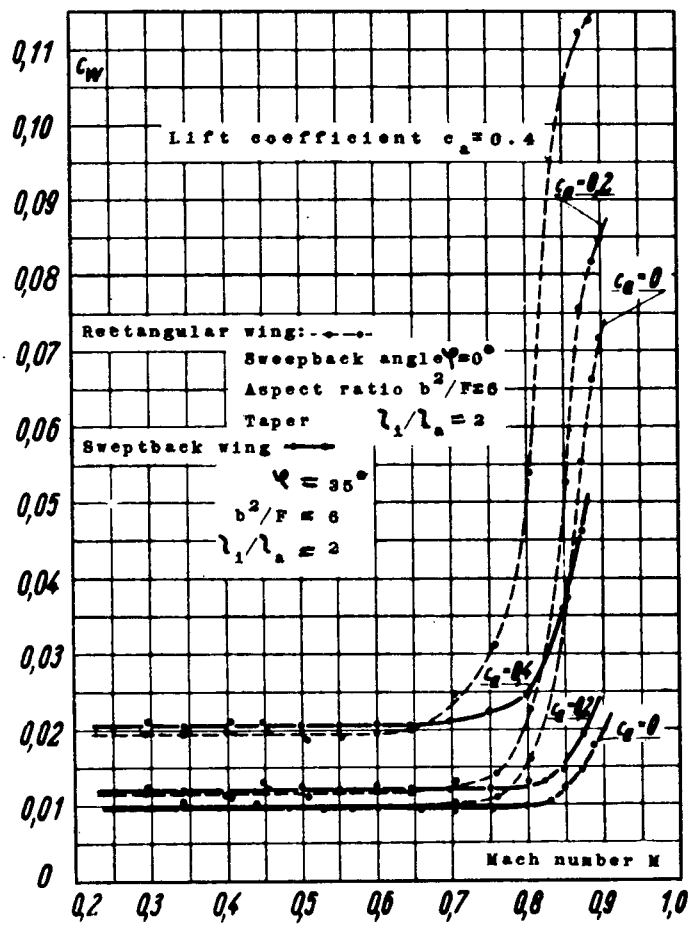

Figure 8. Drag coefficient of a rectangular wing and of a sweptbac wing as a function of the Mach number.

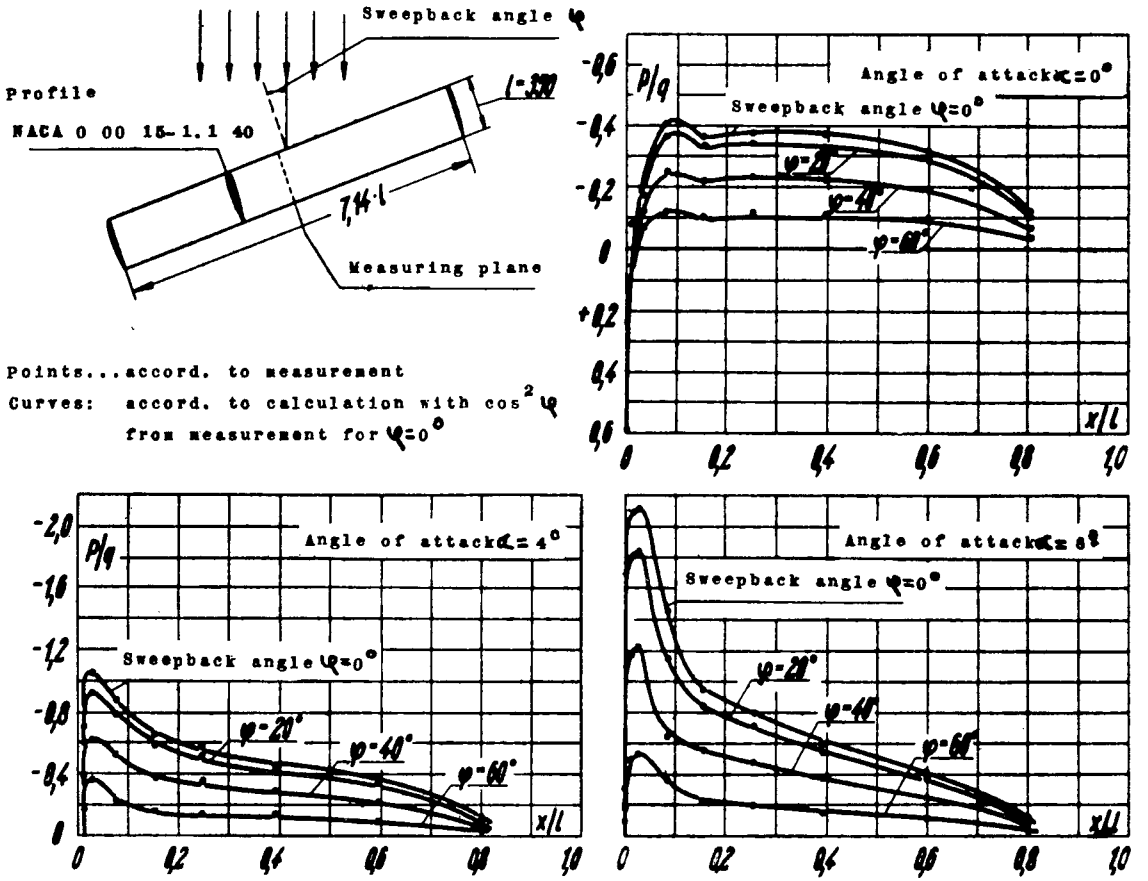

Figure 9. Influence of using sweepback on the pressure distribution at small velocity.

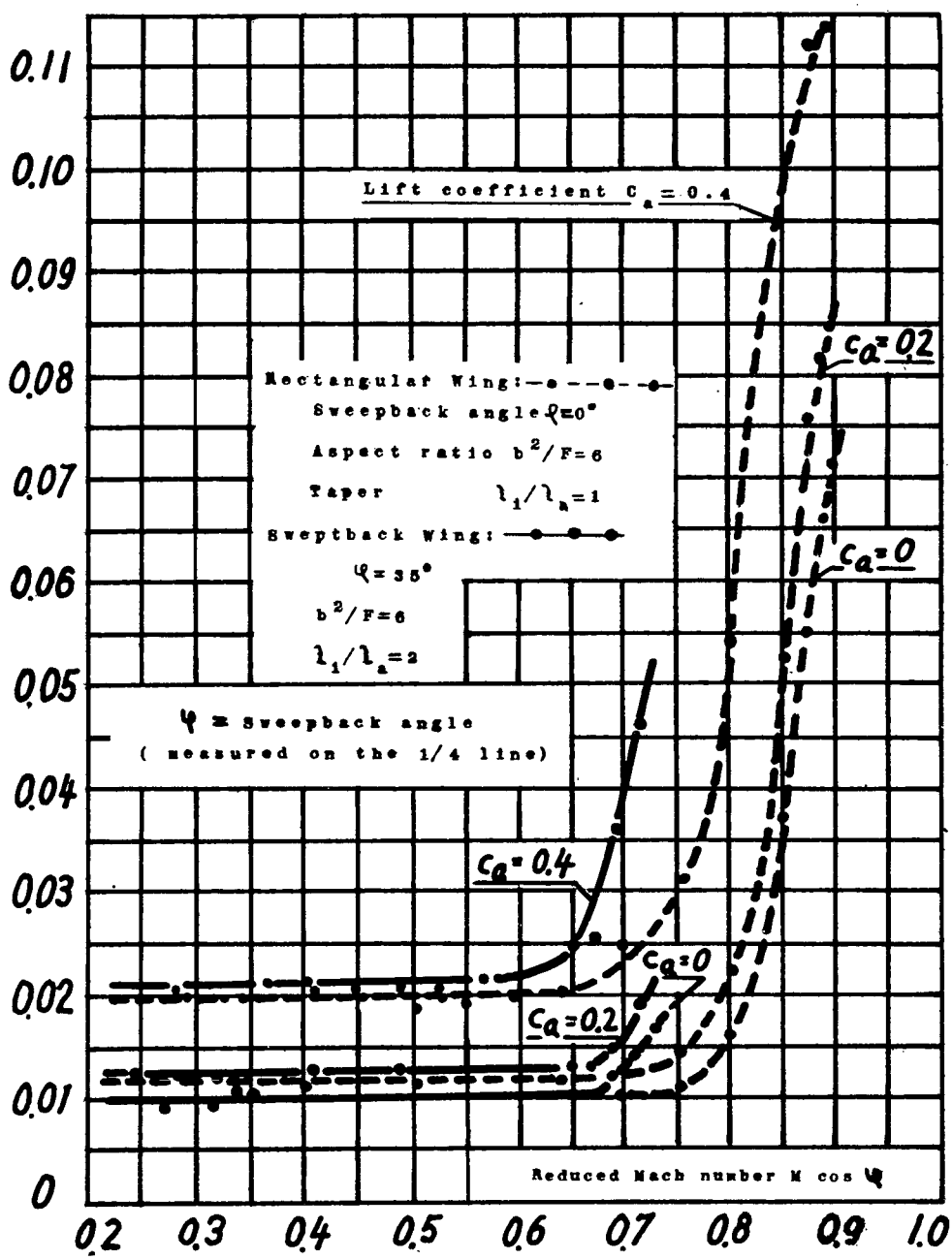

Figure 10. Drag coefficient of a rectangular wing and of a sweptback wing as a function of the reduced Mach number M cos φ

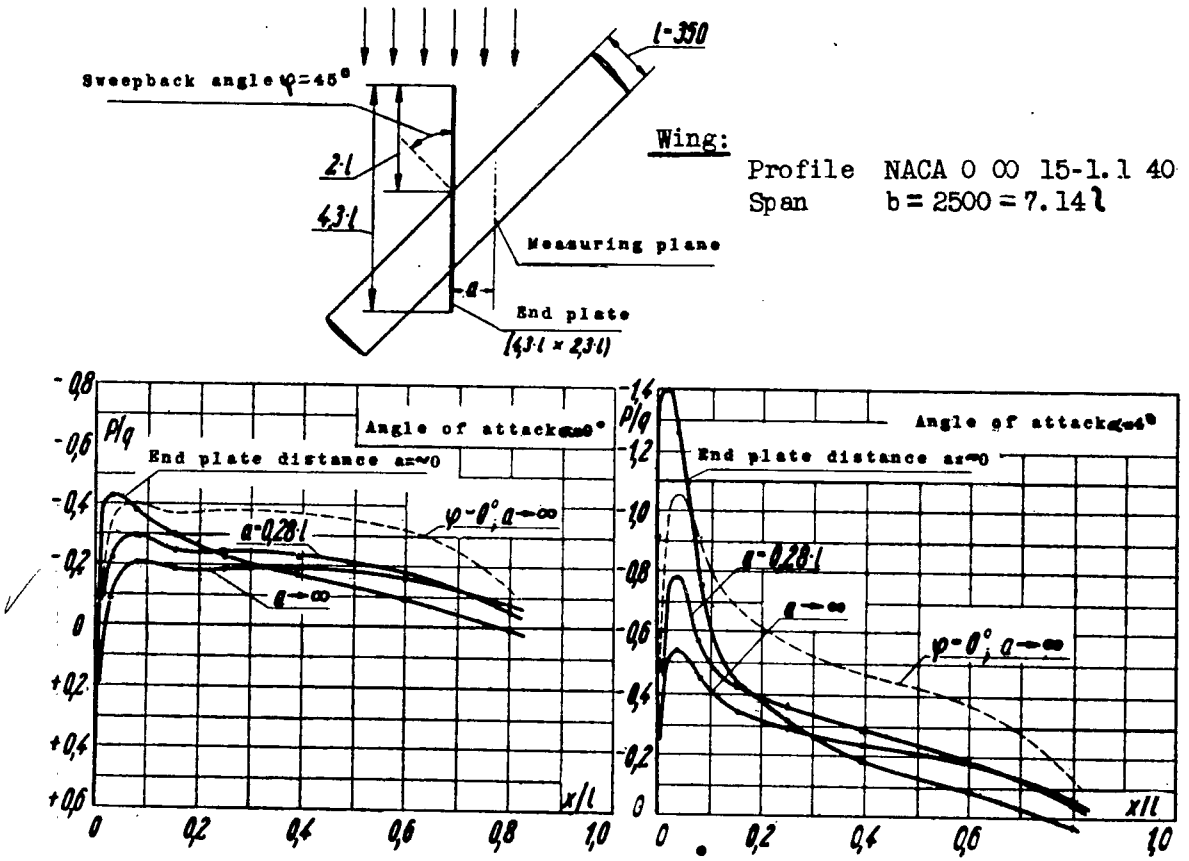

Figure 11. Influence of an end plate on the pressure distribution of a wing with a sweepback angle of 45° (small flow velocity).

Model wing:

Sweepback angle $\varphi = 35^{\circ}$

Aspect ratio $b^2/F = 6$

Taper $l_1/l_a = 2$

Profile NACA 0 00 12-1.1 30

Position of measuring rake:

Distance behind 1/4 line of equival. rectangular wing

$x \doteq \sim 5.31_1$

Distance from center = z

$$f(M) = \frac{c_w}{c_{wges}} = 0.03 = \text{Factor}$$

for consideration of compressibility

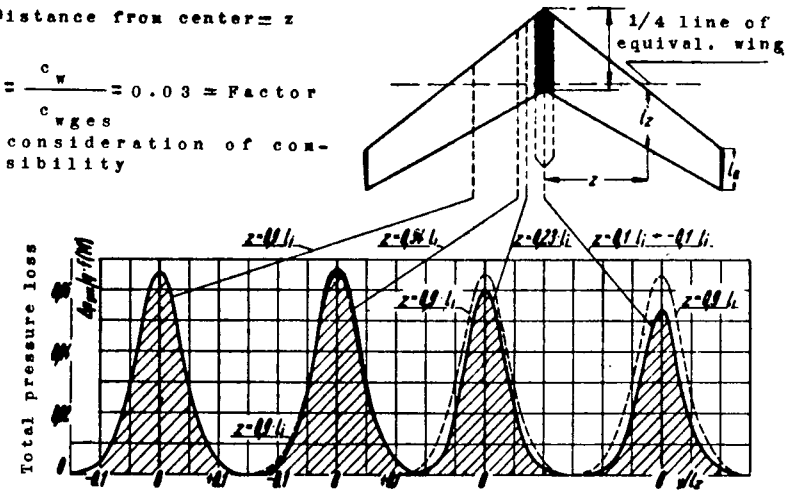

Figure 12. Curves of total head loss of a sweptback wing in different distances from the wing center at the Mach number M = 0,65 (α=0).

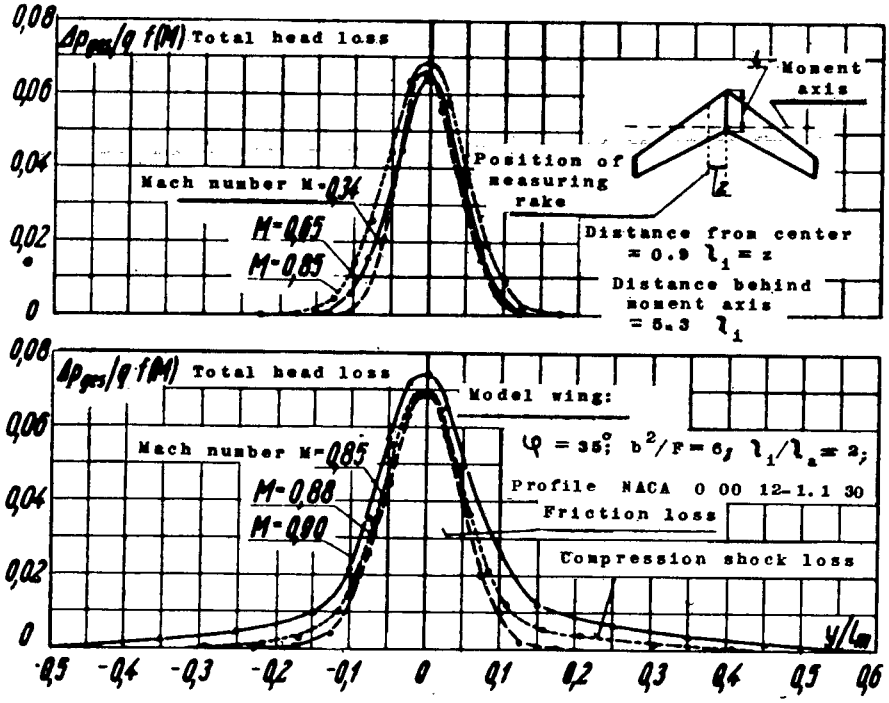

Figure 13. Total head loss behind a sweptback wing (distance of the plane of measurement from wing center $0,9 \cdot \bar{l}_i$ ($\alpha = 0°$).

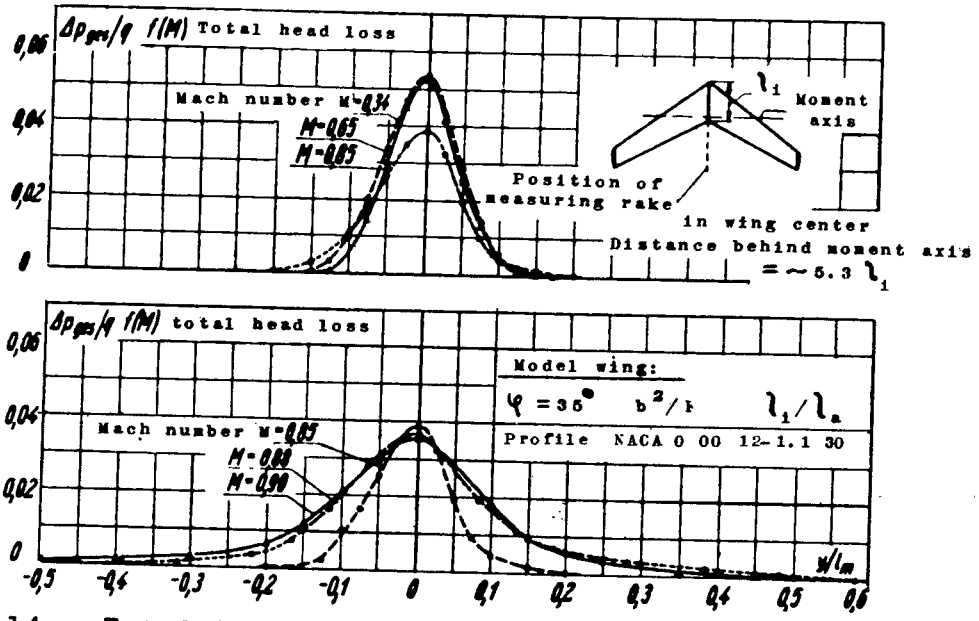

Figure 14. Total head loss behind a sweptback wing (position of measuring rake in wing center) ($\alpha = 0°$).

Model Wing:

sweepback angle $\varphi = 35^\circ$
aspect ratio $b^2/F = 6$
taper $l_i/l_a = 2$

profile: NACA 0 00 12-1.1 30

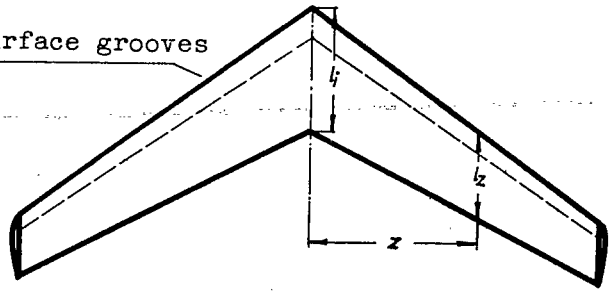

Mach number M=0,86 M=0,87 M=0,89

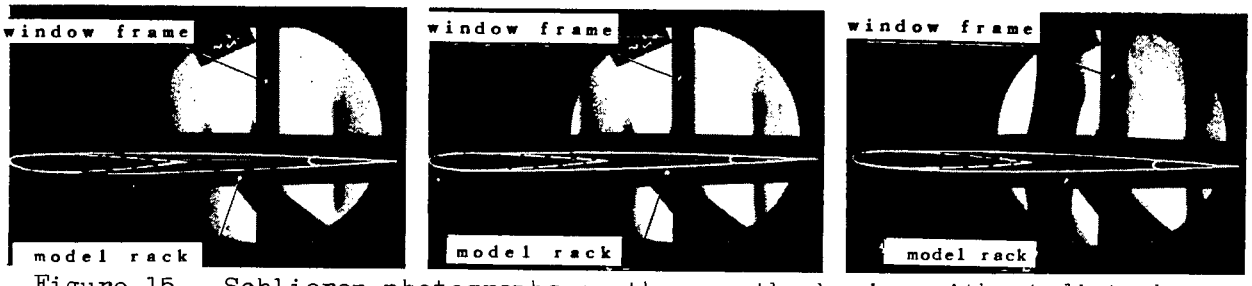

Figure 15. Schlieren photographs cn the sweptback wing without disturbance grooves at different Mach numbers ($\alpha = 0^\circ$)

Model Wing:

sweepback angle $\varphi = 35^\circ$
aspect ratio $b^2/F = 6$
taper $l_i/l_a = 2$

profile: NACA 0 00 12-1.1 30

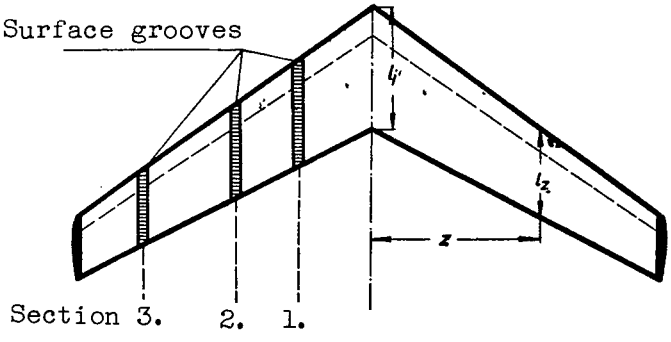

Section 1. distance from center $z = 0{,}56 \cdot l_i$ Section 2. $z = 1{,}05 \cdot l_i$ Section 3. $z = 1{,}79 \cdot l_i$

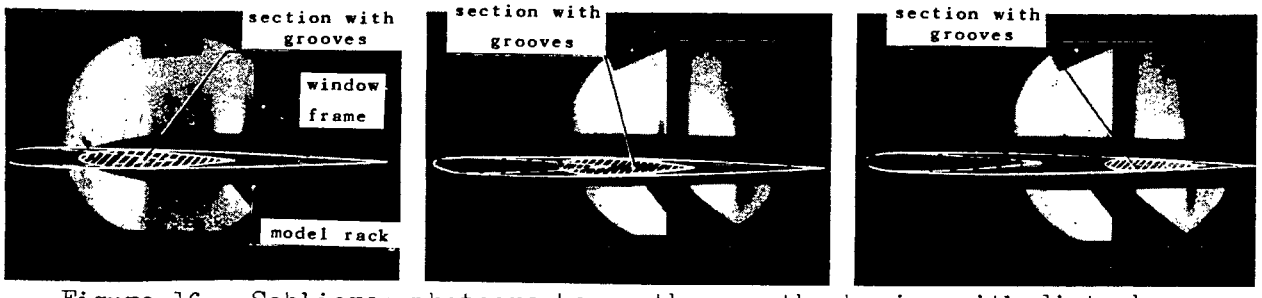

Figure 16. Schlieren photographs on the sweptback wing with disturbance grooves, Mach number =0,85 ($\alpha = 0^\circ$)

Model Wing:

sweepback angle $\varphi = 35^\circ$
aspect ratio $b^2/F = 6$
taper $l_i/l_a = 2$
profile: NACA 0 00 12-1.1 30

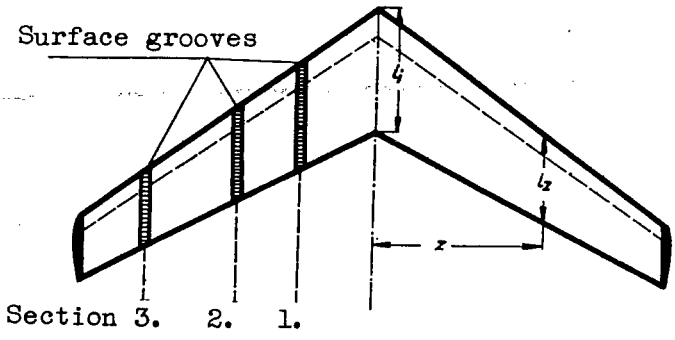

Section 1. distance from center $z = 0{,}56 \cdot l_i$ Section 2. $z = 1{,}05 \cdot l_i$ Section 3. $z = 1{,}79 \cdot l_i$

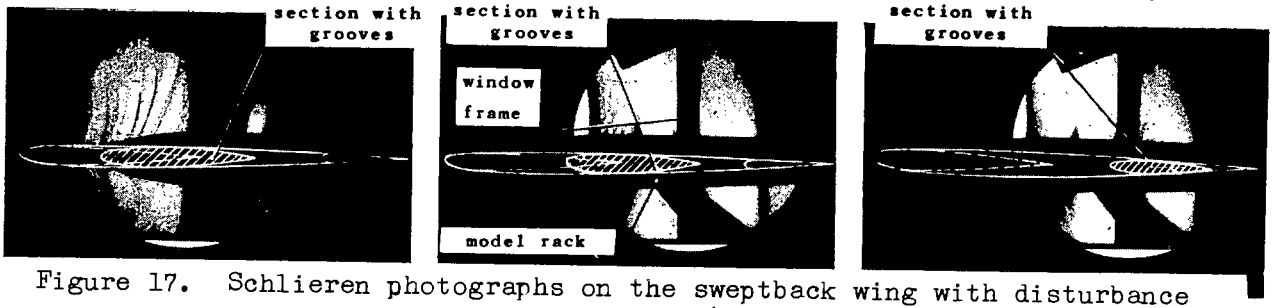

Figure 17. Schlieren photographs on the sweptback wing with disturbance grooves, Mach number M=0,875 ($\alpha = 0^\circ$)

Model Wing:

sweepback angle $\varphi = 35^\circ$
aspect ratio $b^2/F = 6$
taper $l_i/l_a = 2$

profile: NACA 0 00 12-1.1 30

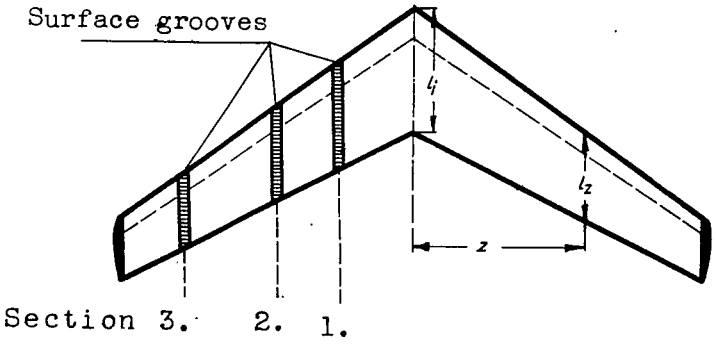

Section 1. distance from center $z = 0{,}56 \cdot l_i$ Section 2. $z = 1{,}05 \cdot l_i$ Section 3. $z = 1{,}79 \cdot l_i$

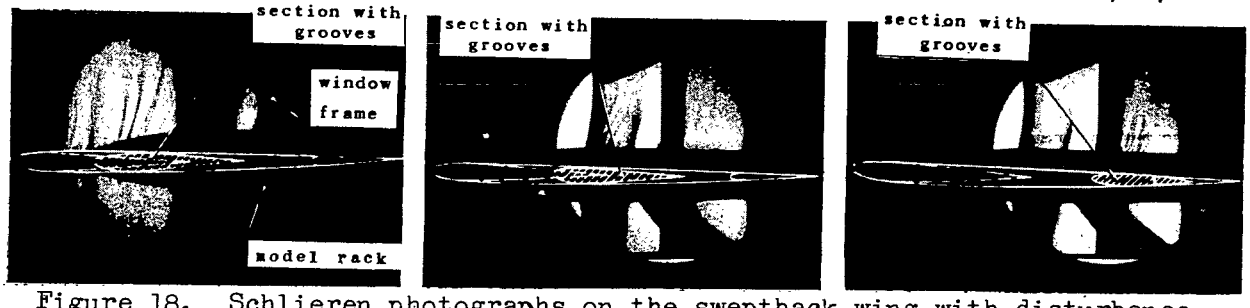

Figure 18. Schlieren photographs on the sweptback wing with disturbance grooves, Mach number M=0,89 ($\alpha = 0^\circ$)

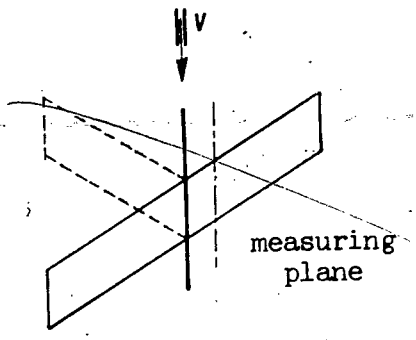

Figure 1.

In connection with a center wall the forward lying half of the oblique wing corresponds to the forward swept wing.

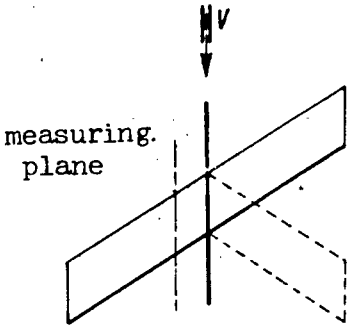

Figure 2.

The rearward lying half of the oblique wing is analogous to the rearward swept wing.

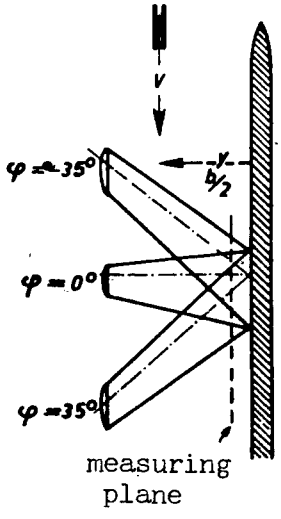

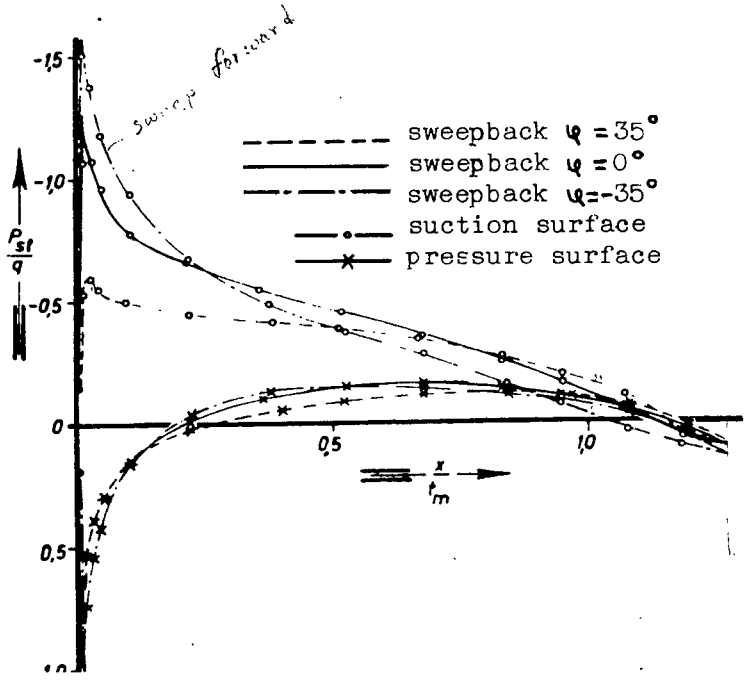

Figure 3. The curves of pressure distribution were measured by Luetgebrune (FB 1501). The distance of the measuring plane from the wall was: $\frac{2y}{b} = 0.056$